View metadata, citation and similar papers at core.ac.uk

brought to you by CORE

provided by Institute of Transport Research:Publications

Remote sensing of mineral dust over land with MSG infrared channels

L. Klüser [1,2] , K. Schepanski[3,4], T. Holzer-Popp [1] , A. Hartmann[1,2]

[1] German Aerospace Center, German Remote Sensing Datacenter (DLR-DFD), Wessling, Germany

[2] University of Augsburg, Institute of Physics, Augsburg, Germany

[3] Leibniz Institute for Tropospheric Research (IfT), Leipzig, Germany

[4] Leibniz-Institute of Marine Sciences (IFM-GEOMAR), Kiel, Germany

lars.klueser@dlr.de

GERMAN REMOTE SENSING DATACENTER

Introduction

Remote sensing of mineral dust optical depth from passive satellite instruments is quite well established over dark surfaces as ocean or vegetation. Over bright reflecting surfaces like deserts radiance observations in shortwave (blue to ultraviolet) and thermal infrared wavelength bands can be used to infer information about airborne mineral dust. In most existing dust detection strategies for thermal infrared observations assumptions of clearsky brightness temperatures are made from prior observations with a time lag of days to weeks. In contrast to this approach the presented new method for dust detection with Meteosat Second Generation (MSG) thermal infrared observations uses the differences in day and night observations in two split-window wavelength bands between dusty and dustfree conditions for the detection of airborne dust. The magnitude of this new dust index can be regarded as an indicator of the atmospheric dust load.

Bitemporal Mineral Dust Index

From daily MSG-SEVIRI $T_{10.8}$ and $T_{12.0}$ brightness temperatures at 03:00 UTC (night) and 12:00 UTC (day) the ***Bitemporal Mineral Dust Index*** (Klüser and Schepanski, 2008, subm. to ACPD) is derived for cloudfree scenes (cloud screening by the Avhrr Processing scheme Over Land, cLouds and Ocean, APOLLO, Kriebel et al., 2003) by the following steps:

$$BTD(t_{1,2}) = T_{10.8}(t_{1,2}) - T_{12.0}(t_{1,2}) \quad (1)$$

$$\Delta T = T_{10.8}(\text{day}) - T_{10.8}(\text{night}) \quad (2)$$

$$\Delta BTD = BTD(\text{day}) - BTD(\text{night}) \quad (3)$$

$N_{APOLLO}=0$ $\Theta_V < 60°$ | BTD < 1K at 03:00 | $T_{10.8} \geq 273K$ at 03:00, 12:00 | BTD < 0K at 12:00

$$BMDI = \Delta BTD + \Delta T_{10.8}/7 \quad (4)$$

Low BMDI values correspond to high atmospheric dust load, besides the particle concentrations the BMDI is also assumed to depend on dust layer height, dust particle size distributions and the chemical composition of the transported dust.

Fig.1 shows the detection of dust storms on 08.03.2006 with the BMDI. For comparison a RGB composite image from MSG infrared observations with $[R,G,B]=[T_{12.0}-T_{10.8}, T_{10.8}-T_{8.7}, T_{10.8}(inv)]$ is also shown.

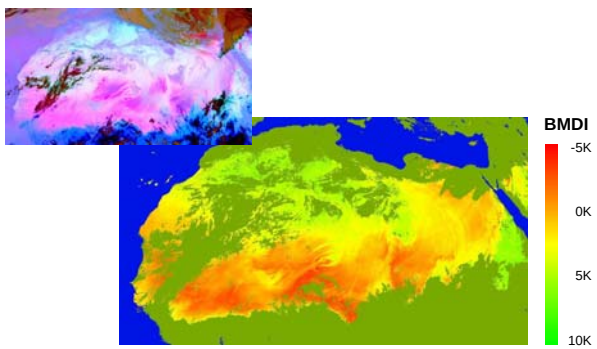

Figure 1: Dust storms over the Sahara domain on 08.03.2006. Large image: BMDI values, small image: „dust" RGB composite with $[R,G,B]=[T_{12.0}-T_{10.8}, T_{10.8}-T_{8.7}, T_{10.8}(inv)]$.

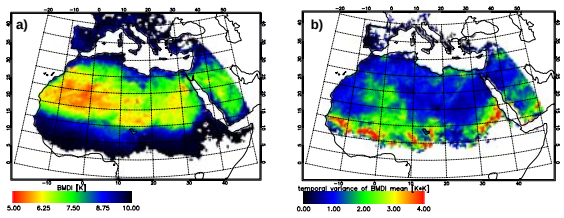

Figure 2: Mean values (a) and temporal variance (b) of BMDI observations for the year 2006 mapped onto a 0.5° grid.

Evaluation of the BMDI

In Fig.2 BMDI mean values (a) and temporal variance (b) of 0.5° gridboxes are shown for the year 2006. Mean values are especially high in dust source regions, while variance is highest at the southern end of the Sahara, where heavy northerly dust storms episodically occur.

Fig. 3 shows the comparison of BMDI values with the AERosol RObotic NETwork AERONET (Holben et al.,1998) Aerosol Optical Depth (AOD) for eight stations around the Sahara. The correlation between BMDI and AOD is r=-0.796, symbol colours indicate Ångström exponents as inferred from AERONET observations.

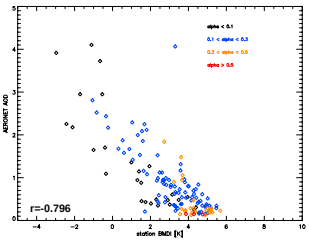

Figure 3: Comparison between AERONET AOD (11-12 UTC average) and BMDI values (3x3 pixel average centered at the station's location) for eight AERONET stations during 2006. α indicates different Ångström exponent classes.

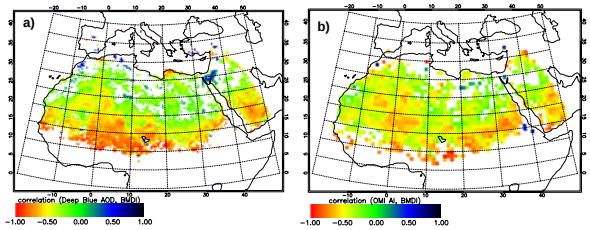

Figure 4: Rank correlations between BMDI and Terra-MODIS Deep Blue AOD (a) and between BMDI and OMI AI (b).

Spearman rank correlations (90% significance) between BMDI and the Terra satellite's MODerate resolution Imaging Spectro-radiometer (MODIS) „Deep Blue" AOD (Hsu et al., 2004), shown in Fig.4a, show good agreement in dust detection between BMDI and Deep Blue (anticorrelated) in the southern part of the Sahara and the main source regions, while in mountainous terrain correlation magnitudes are low (partly due to very small sample sizes). Correlations between BMDI and the Aura satellite's Ozone Monitoring Instrument Absorbing Aerosol Index (OMI AI, Torres et al., 1998) with 1.0° spatial resolution (Fig.4b) show similar patterns, but with overall lower magnitudes due to different height dependence of BMDI and OMI AI and AI sensitivity to biomass burning aerosols.

Fig.5 shows BMDI values (a and b) and mineral dust AOD (c and d) from simulations of the Model of Atmospheric Transport and Chemistry (MATCH) in combination with the Dust Entrainment And Deposition (DEAD) model (Zender et al., 2003) on a 1.9° grid for two subsequent days with dust storms (04./05.03.2004). Those images emphasize the ability to observe dust plume propagation across the Sahara domain with the BMDI.

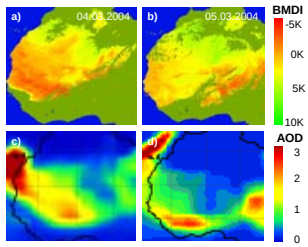

Figure 5: BMDI (a and b) and MATCH-DEAD model AOD (c and d) for the 04./05.03.2004 dust storm.

Summary and conclusions

A new method for the detection of airborne mineral dust from MSG thermal infrared observation is presented. Several lines of evaluation show good results regarding the dust detection ability of this Bitemporal Mineral Dust Index. The BMDI is sensitive to the atmospheric dust load as well. Daily maps of mineral dust load in terms of BMDI can be produced either on the MSG pixel resolution or mapped onto a 0.5° grid. The BMDI method uses the day-night contrast of split-window brightness temperatures and thus is independent from clearsky assumptions inferred from prior observations, which might be affected by different weather conditions or surface temperatures.

In contrast to AOD retrievals from solar radiation observations, the BMDI is insensitive to small-particle aerosols such as from biomass burning.

Acknowledgements

We thank Naif Al-Abbadi, Bernadette Chatenet, Phillipe Goloub, Jean Louis Rajot, Didier Tanré, and Rick Wagener and their staff for establishing and maintaining the eight AERONET sites used in this investigation and for providing the observation data. We acknowledge to the GES-DISC Interactive Online Visualization ANd Analysis Infrastructure (Giovanni) as part of the NASA's Goddard Earth Science (GES) Data and Information Service Center (DISC) for the OMI data set. We thank the MODIS Atmosphere Discipline Group for providing MODIS aerosol data. We also acknowledge to the NASA's Goddard Space Flight Center's Level 1 and Atmosphere Archive and Distribution System (LAADS) for the online distribution of the MODIS data.

References

- Holben, B.N., Eck, T.F., Slutsker, I., Tanré, D., Buis, J.P., Setzer, A., Vermote, E., Reagan, J.A., Kaufman, Y.J., Nakajima, T., Lavenu, F., Jankowiak, I., and Smirnov, A., 1998: AERONET – A federated instrument network and data archive for aerosol characterization, Remote Sens. Environ., 66, 1-16
- Hsu, N.C., Tsay, S.C., King, M.D., and Herman, J.R., 2004: Aerosol Properties Over Bright-Reflecting Source Regions, IEEE T. Geosci. Remote, 42, 557-569
- Kriebel, K.T., Gesell, G., Kästner, M. und Mannstein, H., 2003: The cloud analysis tools APOLLO: improvements and validations, Int. J. Remote Sens., 24, 12, 2389-2408
- Torres, O., Bhartia, P.K., Herman, J.R., Ahmad, Z., and Gleason, J. 1998: Derivation of aerosol properties from a satellite measurements of backscattered ultraviolet radiation: Theoretical basis, J. Geophys. Res., 103, 17099-17110
- Zender, C. S., Bian, H., and Newman, D, 2003: Mineral Dust Entrainment and Deposition (DEAD) model: Description and 1990s dust climatology, J. Geophys. Res., 108(D14), 4416, doi:10.1029/2002JD002775

Deutsches Zentrum für Luft- und Raumfahrt e.V. in der Helmholtz-Gemeinschaft

German Aerospace Center (DLR)
German Remote Sensing Datacenter (DFD)
D-82234 Wessling
Internet: www.dlr.de/caf